Identification of a novel cationic glycolipid in *Streptococcus agalactiae* that contributes to brain entry and meningitis

Luke R. Joyce[a,b], Haider S. Manzer[b], Jéssica da C. Mendonça[b,c], Ricardo Villarreal[b], Prescilla E. Nagao[c] , Kelly S. Doran[b#,] Kelli L. Palmer[a#], and Ziqiang Guan[d#]

[a]Department of Biological Sciences, The University of Texas at Dallas, Richardson, TX, 75080

[b]Department of Immunology and Microbiology, University of Colorado School of Medicine, Aurora, CO, 80045

[c]Rio de Janeiro State University, Roberto Alcântara Gomes Biology Institute, Rio de Janeiro, RJ, Brazil

[d]Department of Biochemistry, Duke University Medical Center, Durham, NC, 27710

Short title: GBS MprF synthesizes a novel glycolipid that contributes to meningitis

#Corresponding authors

Kelly S. Doran: Kelly.Doran@CUAnschutz.edu

Kelli L. Palmer: Kelli.Palmer@UTDallas.edu

Ziqiang Guan: Ziqiang.Guan@Duke.edu

Keywords: Group B *Streptococcus*, Lipidomics, Glycolipid, Meningitis, MprF

Abstract

Bacterial membrane lipids are critical for membrane bilayer formation, cell division, protein localization, stress responses, and pathogenesis. Despite their critical roles, membrane lipids have not been fully elucidated for many pathogens. Here, we report the discovery of a novel cationic glycolipid, Lysyl-Glucosyl-Diacylglycerol (Lys-Glc-DAG) that is synthesized in high abundance by the bacterium *Streptococcus agalactiae* (Group B *Streptococcus*, GBS). To our knowledge, Lys-Glc-DAG is more positively charged than any other known lipids. Lys-Glc-DAG carries two positive net charges per molecule, distinct from the widely described lysylated phospholipid Lysyl-phosphatidylglycerol (Lys-PG) which carries one positive net charge due to the presence of a negatively charged phosphate moiety. We use normal phase liquid chromatography (NPLC) coupled with electrospray ionization (ESI) high-resolution tandem mass spectrometry (HRMS/MS) and genetic approaches to determine that Lys-Glc-DAG is synthesized by the enzyme MprF in GBS, which covalently modifies the neutral glycolipid Glc-DAG with the cationic amino acid lysine. GBS is a leading cause of neonatal meningitis, which requires traversal of the endothelial blood-brain barrier (BBB). We demonstrate that GBS strains lacking *mprF* exhibit a significant decrease in the ability to invade BBB endothelial cells. Further, mice challenged with a GBS∆*mprF* mutant developed bacteremia comparably to Wild-Type infected mice yet had less recovered bacteria from brain tissue and a lower incidence of meningitis. Thus, our data suggest that Lys-Glc-DAG may contribute to bacterial uptake into host cells and disease progression. Importantly, our discovery provides a platform for further study of cationic lipids at the host-pathogen interface.

47 **Introduction**

48 Bacterial cellular membranes are dynamic structures that are critical for survival under
49 varying environmental conditions and are essential for host-pathogen interactions.
50 Phospholipids and glycolipids within the membrane have varying chemical properties that
51 alter the physiology of the membrane, which bacteria can modulate in response to
52 environmental stresses such as pH (1), antibiotic treatment (2), and human metabolites
53 (3). Despite their critical roles in the survival and pathogenesis, membrane lipids have not
54 been carefully characterized using modern lipidomic techniques for many important
55 human pathogens, including *Streptococcus agalactiae* (Group B *Streptococcus*; GBS).
56 GBS colonizes the lower genital and gastrointestinal tracts of ~30% of healthy women (4,
57 5). However, GBS can cause sepsis and pneumonia in newborns and is a leading cause
58 of neonatal meningitis, resulting in long-lasting neurological effects in survivors (6-8). Due
59 to the severity of the resulting diseases, intrapartum antibiotic prophylaxis is prescribed
60 for colonized pregnant women (7, 9). Even with these measures, a more complete
61 understanding of GBS pathogenesis and new therapeutic and preventive measures are
62 needed to mitigate the devastating impact of GBS neonatal infection.

63

64 Research on the pathogenesis of the GBS has mainly focused on cell wall-anchored or
65 secreted proteins and polysaccharides that aid in the attachment to and invasion of host
66 cells. The numerous attachment and virulence factors possessed by the GBS are
67 summarized in a recent review by Armistead *et al* 2019 (10). Comparatively little is known
68 about GBS cellular membrane lipids. To our knowledge, the only characterization of GBS
69 lipids prior to our current study was the identification of the phospholipids

70 phosphatidylglycerol (PG), cardiolipin (CL), and lysyl-phosphatidylglycerol (Lys-PG) in
71 GBS (11-13). Similarly, investigation into the glycolipids of the GBS membrane has
72 focused on di-glucosyl-diacylglycerol (Glc_2-DAG), which is the lipid anchor of the Type I
73 lipoteichoic acid, and its role in pathogenesis (14).
74
75 In this study, we utilized normal phase liquid chromatography (NPLC) coupled with
76 electrospray ionization (ESI) high-resolution tandem mass spectrometry (HRMS/MS) to
77 characterize the GBS membrane lipid composition, and identified a novel cationic
78 glycolipid, lysyl-glucosyl-diacylglycerol (Lys-Glc-DAG), which comprises a major portion
79 of the GBS total lipid extract. While Lys-PG has been reported in a range of bacterial
80 species (15), Lys-Glc-DAG represents, to our knowledge, the first example of lysine
81 modification of a neutral glycolipid. By gene deletion and heterologous expression, we
82 show the GBS MprF enzyme is responsible for the biosynthesis of both the novel Lys-
83 Glc-DAG and Lys-PG. Most strikingly, using an *in vivo* hematogenous murine infection
84 model, we demonstrate that MprF does not contribute to GBS bloodstream survival. This
85 distinguishes the GBS MprF from the well-known *Staphylococcus aureus* MprF, which
86 synthesizes only Lys-PG (16, 17). Rather, GBS MprF contributes specifically to meningitis
87 and penetration of the blood-brain barrier. These results greatly expand our knowledge
88 of naturally occurring lipids and MprF functionality and reveal insights into the
89 pathogenesis of meningitis caused by GBS.
90
91 **Results**
92 **Identification of Lys-Glc-DAG, a novel cationic glycolipid in GBS**

93 The membrane lipids of three GBS clinical isolates of representative serotypes were
94 characterized: COH1 (18), A909 (19), CNCTC 10/84 and CJB111 (20) (serotypes III, 1a,
95 and V, respectively). Common Gram-positive bacterial lipids were identified by normal
96 phase LC coupled with negative ion ESI/MS/MS, including diacylglycerol (DAG),
97 monohexosyldiacylglycerol (MHDAG), dihexosyldiacylglycerol (DHDAG),
98 phosphatidylglycerol (PG), and lysyl-phosphatidylglycerol (Lys-PG), as shown by the
99 negative total ion chromatogram (TIC) (Fig. 1A).
100
101 Surprisingly, the positive TIC (Fig. 1B, S1 Fig) shows highly abundant peaks of unknown
102 identity at the retention time ~25-29 min. The mass spectra (Fig. 1C) and LC retention
103 times of this lipid do not match with any other bacterial lipids we have analyzed or exact
104 masses in lipidomic databases (21, 22). Tandem MS (MS/MS) in the positive ion mode
105 (Fig. 1D), negative ion mode (Fig. 1E), and high-resolution mass measurement (Fig. 1C)
106 allowed us to propose lysyl-glucosyl-diacylglycerol (Lys-Glc-DAG) (Fig. 1F) as the
107 structure of this unknown lipid. Observed and exact masses of Lys-Glc-DAG are shown
108 in S1 Table. The assignment of glucose was based on the observation that glucosyl-
109 diacylglycerol (Glc-DAG) is a major membrane component of GBS and other streptococci
110 (14), and results from an isotopic labeling experiment using ^{13}C-labeled glucose
111 (Glucose-$^{13}C_6$). The assignment of lysine modification was supported by an isotopic
112 labeling experiment with deuterated lysine (lysine-*d4*). The expected mass shifts (+4 Da)
113 were observed in both molecular ions and MS/MS product ions (S2 Fig). Comparison of
114 both MS/MS spectra of labeled (Glucose-$^{13}C_6$) and unlabeled Lys-Glc-DAG indicates the
115 lysine residue is linked to the 6-position of glucose (S2 Fig). Lys-Glc-DAG consists of

116 several molecular species with different fatty acyl compositions resulting in different
117 retention times and multiple, unresolved TIC peaks (~25-29 min).
118
119 **GBS MprF synthesizes Lys-Glc-DAG**
120 The enzyme MprF (multiple peptide resistance factor) catalyzes the aminoacylation of PG
121 with lysine in some Gram-positive pathogens (16, 23). We determined that GBS MprF is
122 responsible and sufficient for synthesizing Lys-Glc-DAG as well as Lys-PG. Deletion of
123 *mprF* from both COH1 and CJB111 abolishes Lys-Glc-DAG and Lys-PG synthesis, which
124 are restored by complementation (Fig. 1G, S3 Fig). Deletion of GBS *mprF* does not confer
125 a growth defect in Todd-Hewitt broth or tissue culture medium. The oral colonizer
126 *Streptococcus mitis* does not encode *mprF* or synthesize Lys-PG but synthesizes Glc-
127 DAG and PG (2, 3). Heterologous expression of GBS *mprF* in *S. mitis* results in Lys-Glc-
128 DAG and Lys-PG production (Fig. 1H), while expression of *Enterococcus faecium mprF*
129 results in only Lys-PG production (Fig. 1H), as expected (1). Biosynthetic pathways
130 involving MprF are shown in Fig. 1I.
131
132 **MprF contributes to GBS pathogenesis**
133 We investigated whether MprF contributes to GBS invasion into brain endothelial cells
134 and development of meningitis. To mimic the human blood-brain barrier (BBB), we utilized
135 the human cerebral microvascular endothelial cell line hCMEC/D3. *In vitro* assays for
136 adhesion and invasion were performed as described previously (14, 24, 25). There was
137 no significant difference in the ability of Δ*mprF* compared to WT and complement cells to
138 attach to hCMEC/D3 cells (Fig. 2A). However, we observed a significant decrease in the

139 amount of Δ*mprF* recovered from the intracellular compartment of hCMEC/D3 cells (Fig.
140 2A). The reduced invasion phenotype was confirmed in the hypervirulent serotype V
141 strain, CJB111 (26, 27) (S4 Fig). Intracellular survival requires GBS to survive low pH
142 conditions in lysosomes (pH 4.5 – 5.5) (28), and Δ*mprF* is unable to survive low pH
143 conditions (Fig. 2B). This suggests that MprF promotes GBS invasion and possibly
144 intracellular survival in brain endothelial cells.
145
146 We hypothesized that these *in vitro* phenotypes of Δ*mprF* would translate into a
147 diminished ability to penetrate the BBB and produce meningitis *in vivo*. Using our
148 standard model of GBS hematogenous meningitis (14, 24) mice were challenged with
149 either WT GBS or Δ*mprF*. Mice were sacrificed at 72 h to determine bacterial loads in
150 blood, lung and brain tissue. We recovered significantly less CFU in the brains of Δ*mprF*-
151 infected mice compared to the WT-infected mice (Fig. 2C). However, there was no
152 significant difference in CFU recovered from the bloodstream or the lung (Fig. 2D,E),
153 demonstrating that Δ*mprF* does not have a general defect in bloodstream survival or
154 tissue invasion *in vivo*. Furthermore, mice challenged with WT GBS had significantly more
155 meningeal thickening and neutrophil chemokine, KC, in brain homogenates compared to
156 Δ*mprF* mutant-infected animals (Fig. 2F-H). Taken together, *mprF* contributes to GBS
157 penetration into the brain and to the pathogenesis of meningitis *in vivo*.
158
159 **Discussion**
160 Here, we report that GBS MprF uniquely synthesizes a novel cationic glycolipid Lys-Glc-
161 DAG in high abundance plays a role in the invasion of human endothelial cells. This work

162 establishes that GBS capitalizes on MprF to modulate charges of both glycolipids and
163 phospholipids at the membrane, which is unprecedented
164
165 Previously MprF has been shown to catalyze the aminoacylation of the anionic
166 phospholipid PG in a range of Gram-positive and Gram-negative bacteria (16, 23). MprF
167 is a membrane-bound enzyme comprised of a N-terminal lipid flippase domain (29) and
168 a C-terminal catalytic domain that catalyzes the aminoacylation of the glycerol group of
169 PG by using aminoacyl-tRNAs as the amino acid donors (30-32). An important function
170 of PG aminoacylation is proposed to decrease the net negative charge of the cellular
171 envelope to confer protection from cationic antimicrobial peptides (CAMPs) produced by
172 host immune systems and bacteriocins produced by competitor bacteria (16, 23).
173 However, a previous study observed no contribution of *mprF* to GBS *in vitro* susceptibility
174 to commonly studied CAMPs, which is unlike the well-characterized *S. aureus mprF* (33),
175 thus highlighting the unique differences between the extracellular surface of these
176 bacteria.
177
178 Based on our tissue culture and mouse infection experiments, we propose that GBS have
179 an MprF enzyme and corresponding cellular lipid properties that are adapted for efficient
180 invasion of mammalian cells. Deletion of *mprF* impacts the ability of GBS to enter the
181 brain and promote meningitis *in vivo*. This suggests that MprF plays a role in BBB
182 penetration and not invasion into the lung, however additional studies are warranted to
183 examine other tissue sites. It is unknown how lysinylated lipids in the GBS membrane,
184 which is covered by a layer of peptidoglycan, mechanistically impact invasion. Because

185 Lys-Glc-DAG is abundantly synthesized by GBS MprF, with Lys-PG a comparatively
186 minor product, it is likely that Lys-Glc-DAG is the most relevant lipid for meningitis
187 pathogenesis. Speculatively, Lys-Glc-DAG may contribute to membrane vesicle (MV)
188 formation by GBS. MVs have previously been shown to be pro-inflammatory and result
189 in preterm birth and fetal death in mice (34), but have not been studied during meningitis
190 progression. In future studies, it will be key to investigate this, as well as the specific host
191 inflammatory and signaling responses to the GBS *mprF* mutant.
192
193 Our identification of the novel Lys-Glc-DAG glycolipid rationalizes further study of the
194 lipidomes of human pathogens. First, lipids contribute to virulence, and understanding
195 these virulence mechanisms and the mechanisms for lipid synthesis may identify novel
196 antimicrobial drug targets. The decreased *in vivo* pathogenicity of the Δ*mprF* mutant
197 identifies GBS MprF as a candidate for targeting by antimicrobial strategies. Moreover,
198 Lys-Glc-DAG could be utilized as a specific molecular biomarker for GBS diagnostics. In
199 addition, engineered cationic lipids are utilized in lipid nanoparticles for mRNA vaccine
200 and drug delivery and are required for uptake of particles into cells (35, 36). Substantial
201 effort has been dedicated to the synthesis of cationic lipids with low toxicity and efficient
202 delivery properties. Lys-Glc-DAG is a naturally occurring, strongly cationic lipid with
203 potential for use in lipid nanoparticles for vaccine and drug delivery. Importantly, our
204 discovery suggests that lipidome analysis of human pathogens is likely to reveal novel
205 lipids of biotechnological utility.
206
207 **Materials and methods**

208 **Bacterial strains, media, and growth conditions**

209 See S2 Table for strains used in this study. GBS strains were grown statically at 37°C in
210 Todd-Hewitt Broth (THB) and *S. mitis* strains were grown statically at 37°C and 5% CO_2,
211 unless otherwise stated. Streptococcal chemically defined medium (37) was diluted from
212 stock as described (38) with 1% w/v glucose (referred to as DM), slightly modified from
213 (39), unless otherwise stated. *Escherichia coli* strains were grown in Lysogeny Broth (LB)
214 at 37°C with rotation at 225 rpm. Kanamycin and erythromycin (Sigma-Aldrich) were
215 supplemented to media at 50 µg/mL and 300 µg/mL for *E. coli,* respectively, or 300 µg/mL
216 and 5 µg/mL, respectively, for streptococcal strains.

217

218 **Routine molecular biology techniques**

219 All PCR reactions utilized Phusion polymerase (Thermo Fisher). PCR products and
220 restriction digest products were purified using GeneJET PCR purification kit (Thermo
221 Fisher) per manufacturer protocols. See S3 Table for primers. Plasmids were extracted
222 using GeneJET plasmid miniprep kit (Thermo Fisher) per manufacturer protocols.
223 Restriction enzyme digests utilized XbaI, XhoI, and PstI (New England Biolabs) for 3 h at
224 37°C in a water bath. Ligations utilized T4 DNA ligase (New England Biolabs) at 16°C
225 overnight or Gibson Assembly Master Mix (New England Biolabs) per manufacturer
226 protocols where stated. All plasmid constructs were sequence confirmed by Sanger
227 sequencing (Massachusetts General Hospital DNA Core or CU Anschutz Molecular
228 Biology Core).

229

230 **Deuterated lysine and $^{13}C_6$-D-glucose isotope tracking**

231 A GBS COH1 colony was inoculated into 15 mL of DM containing 450 μM lysine-*d4*
232 (Cambridge Isotopes Laboratories) or a single COH1 colony was inoculated into 10 mL
233 DM supplemented with 0.5% w/v $^{13}C_6$D-glucose (U-13C6, Cambridge Isotopes
234 Laboratories) for overnight growth for lipidomic analysis described below.
235

236 **Construction of MprF expression plasmids**

237 Genomic DNA was isolated using the Qiagen DNeasy Blood and Tissue kit per the
238 manufacturer's protocol with the exception that cells were pre-treated with 180 μL 50
239 mg/mL lysozyme, 25 μL 2500 U/mL mutanolysin, and 15 μL 20 mg/mL pre-boiled RNase
240 A and incubated at 37°C for 2 h. The *mprF* genes from GBS COH1, (GBSCOH1_1931),
241 GBS CJB111 (ID870_10050), and *E. faecium* 1,231,410 (EFTG_00601) were amplified
242 and either Gibson ligated into pABG5Δ*phoZ* (40) or ligated into pDCErm (41). Plasmid
243 constructs were transformed into chemical competent *E. coli*. Briefly, chemically
244 competent cells were incubated for 10 min on ice with 5 μL of Gibson reaction before heat
245 shock at 42°C for 70 sec, then placed on ice for 2 min before 900 μL of cold SOC medium
246 was added. Outgrowth was performed at 37°C, with shaking at 225 rpm, for 1 h. Cultures
247 were plated on LB agar plates containing 50 μg/mL kanamycin. Colonies were screened
248 by PCR for presence of the *mprF* insert.
249

250 **Expression of *mprF* in *S. mitis***

251 Natural transformation was performed as previously described (3). Briefly, precultures
252 were thawed at room temperature, diluted in 900 μL of THB, further diluted 1:50 in
253 prewarmed 5 mL THB, and incubated for 45 min at 37°C. 500 μL of culture was then

254 aliquoted with 1 µL of 1 mg/ml competence-stimulating peptide (EIRQTHNIFFNFFKRR)
255 and 1 µg/mL plasmid. Transformation reaction mixtures were cultured for 2 h at 37°C in
256 microcentrifuge tubes before being plated on THB agar supplemented with 300 µg/mL
257 kanamycin. Single transformant colonies were cultured in 15 mL THB overnight. PCR
258 was used to confirm the presence of the *mprF* insert on the plasmid. Plasmids were
259 extracted and sequence confirmed as described above. Lipidomics was performed as
260 described below in biological triplicate.
261

262 **Construction of *mprF* deletion plasmids**

263 Regions ~2 kb upstream and downstream of the GBS COH1 *mprF* (GBSCOH1_1931) or
264 CJB111 (ID870_10050) were amplified using PCR. Plasmid, pMBSacB (42), and the
265 PCR products were digested using appropriate restriction enzymes and ligated overnight.
266 7 µL of the ligation reaction was transformed into chemically competent *E. coli* DH5α as
267 described above, except that outgrowth was performed at 28°C with shaking at 225 rpm
268 for 90 min prior to plating on LB agar supplemented with 300 µg/mL erythromycin. Plates
269 were incubated at 28°C for 72 h. Colonies were screened by PCR for correct plasmid
270 construction. Positive colonies were inoculated into 50 mL LB media containing antibiotic
271 and incubated at 28°C with rotation at 225 rpm for 72 h. Cultures were pelleted using a
272 Sorvall RC6+ centrifuge at 4,280 x *g* for 6 min at room temperature. Plasmid was
273 extracted as described above except the cell pellet was split into 5 columns to prevent
274 overloading and serial eluted into 50 µL. Plasmid construction was confirmed via
275 restriction digest using XhoI and XbaI, and the insert was PCR amplified and sequence-
276 verified.

277

278 **Generation of electrocompetent GBS cells for *mprF* knockout**

279 Electrocompetent cells were generated as described (42) with minor modifications.
280 Briefly, a GBS COH1 or CJB111 colony was inoculated in 5 mL M17 medium (BD Bacto)
281 with 0.5% glucose and grown overnight at 37°C. The 5 mL was used to inoculate a second
282 overnight culture of 50 mL pre-warmed filter-sterilized M17 medium containing 0.5%
283 glucose, 0.6% glycine, and 25% PEG 8000. The second overnight was added to 130 mL
284 of the same medium and grown for 1 h at 37°C. Cells were pelleted at 3,200 x *g* in a
285 Sorvall RC6+ at 4°C for 10 min. Cells were washed twice with 25 mL cold filter-sterilized
286 GBS wash buffer containing 25% PEG 8000 and 10% glycerol in water, and pelleted as
287 above. Cell pellets were re-suspended in 1 mL GBS wash buffer and either used
288 immediately for transformation or stored in 100 µL aliquots at -80°C until use.

289

290 **Deletion of GBS COH1 and CJB111 *mprF***

291 Electrocompetent cells were generated as described (42) with minor modifications. The
292 double crossover homologous recombination knockout strategy was performed as
293 described previously (25, 42, 43) with minor modifications. 1 µg of plasmid was added to
294 electrocompetent GBS cells and transferred to a cold 1 mm cuvette (Fisher or BioRad).
295 Electroporation was carried out at 2.5 kV on an Eppendorf eporator. 1 mL of THB
296 containing 12.5% PEG 8000, 20 mM $MgCl_2$, and 2 mM $CaCl_2$ was immediately added
297 and then the entire reaction was transferred to a glass culture tube. Outgrowth was at
298 28°C for 2 h followed by plating on THB agar supplemented with 5 µg/mL erythromycin.
299 Plates were incubated for 48 h at 28°C. A single colony was cultured overnight in 5 mL

300 THB with 5 µg/mL erythromycin at 28°C. The culture was screened via PCR for the
301 plasmid insert with the initial denaturing step extended to 10 min. The overnight culture
302 was diluted 1:1000 THB containing 5 µg/mL erythromycin and incubated overnight at
303 37°C to promote single cross over events. The culture was then serial diluted and plated
304 on THB agar plates with antibiotic and incubated at 37°C overnight. Colonies were
305 screened for single crossover events by PCR. Single crossover colonies were inoculated
306 in 5 mL THB at 28°C to promote double crossover events. Overnight cultures were diluted
307 1:1000 into 5 mL THB containing sterile 0.75 M sucrose and incubated at 37°C. Overnight
308 cultures were serial diluted and plated on THB agar and incubated at 37°C overnight.
309 Colonies were patched onto THB agar with and without 5 µg/mL erythromycin to confirm
310 loss of plasmid. Colonies were also screened by PCR for the loss of *mprF*. Colonies
311 positive for the loss of *mprF* were inoculated into 5 mL THB at 37°C. Cultures were
312 stocked and gDNA extracted as described above, with minor modifications. Sequence
313 confirmation of the *mprF* knockout was done via Sanger sequencing (Massachusetts
314 General Hospital DNA Core or CU Anschutz Molecular Biology Core). The mutant was
315 grown overnight in 15 mL THB at 37°C and pelleted at 6,150 x *g* for 5 min in a Sorvall
316 RC6+ centrifuge at room temperature for lipid extraction as described. Genomic DNA of
317 COH1Δ*mprF* was isolated as described above and whole genome sequencing was
318 performed in paired-end reads (2 by 150 bp) on the Illumina NextSeq 550 platform at the
319 Microbial Genome Sequencing Center (Pittsburgh, PA). Illumina sequence reads are
320 deposited in the Sequence Read Archive, accession PRJNA675025.
321
322 **Complementation of *mprF* in COH1Δ*mprF* and CJB111Δ*mprF***

323 Electrocompetent GBS strains were generated as previously described (44). Briefly,
324 GBSΔ*mprF* was inoculated into 5 mL THB with 0.6% glycine and grown overnight. The
325 culture was expanded to 50 mL in pre-warmed THB with 0.6% glycine and grown to an
326 OD_{600} nm of 0.3 and pelleted for 10 min at 3200 x *g* at 4°C in a Sorvall RC6+ floor
327 centrifuge. The pellet was kept on ice through the remainder of the protocol. The pellet
328 was washed twice with 25 mL and once with 10 mL of cold 0.625 M sucrose and pelleted
329 as above. The cell pellet was resuspended in 400 µL of cold 20% glycerol, aliquoted in
330 50 µL aliquots, and used immediately or stored at -80°C until use. Electroporation was
331 performed as described above, with recovery in THB supplemented with 0.25 M sucrose,
332 and plated on THB agar with kanamycin at 300 µg/mL.
333
334 **Acidic Bligh-Dyer extractions**
335 Centrifugation was performed using a Sorvall RC6+ centrifuge. Cultures were pelleted at
336 4,280 x *g* for 5 min at room temperature unless otherwise stated. The supernatants were
337 removed, and cell pellets were stored at -80°C until acidic Bligh-Dyer lipid extractions
338 were performed as described (3). Briefly, cell pellets were resuspended in 1X PBS
339 (Sigma-Aldrich) and transferred to Coring Pyrex glass tubes with PTFR-lined caps
340 (VWR), followed by 1:2 vol:vol chloroform:methanol addition. Single phase extractions
341 were vortexed periodically and incubated at room temperature for 15 minutes before 500
342 x *g* centrifugation for 10 min. A two-phase Bligh-Dyer was achieved by addition of 100 µL
343 37% HCl, 1 mL $CHCl_3$, and 900 µl of 1X PBS, which was then vortexed and centrifuged
344 for 5 min at 500 x *g.* The lower phase was removed to a new tube and dried under nitrogen
345 before being stored at -80°C prior to lipidomic analysis.

346

347 **Liquid Chromatography/Electrospray Ionization Mass Spectrometry**

348 Normal phase LC was performed on an Agilent 1200 quaternary LC system equipped
349 with an Ascentis silica HPLC column (5 µm; 25 cm by 2.1 mm; Sigma-Aldrich) as
350 described previously (45, 46). Briefly, mobile phase A consisted of chloroform-methanol-
351 aqueous ammonium hydroxide (800:195:5, vol/vol), mobile phase B consisted of
352 chloroform-methanol-water-aqueous ammonium hydroxide (600:340:50:5, vol/vol), and
353 mobile phase C consisted of chloroform-methanol-water-aqueous ammonium hydroxide
354 (450:450:95:5, vol/vol). The elution program consisted of the following: 100% mobile
355 phase A was held isocratically for 2 min, then linearly increased to 100% mobile phase B
356 over 14 min, and held at 100% mobile phase B for 11 min. The LC gradient was then
357 changed to 100% mobile phase C over 3 min, held at 100% mobile phase C for 3 min,
358 and, finally, returned to 100% mobile phase A over 0.5 min and held at 100% mobile
359 phase A for 5 min. The LC eluent (with a total flow rate of 300 µl/min) was introduced into
360 the ESI source of a high-resolution TripleTOF5600 mass spectrometer (Sciex,
361 Framingham, MA). Instrumental settings for negative-ion ESI and MS/MS analysis of lipid
362 species were: IS = -4,500 V, CUR = 20 psi, GSI = 20 psi, DP = -55 V, and FP = -150V.
363 Settings for positive-ion ESI and MS/MS analysis were: IS = +5,000 V, CUR = 20 psi, GSI
364 = 20 psi, DP = +55 V, and FP = +50V. The MS/MS analysis used nitrogen as the collision
365 gas. Data analysis was performed using Analyst TF1.5 software (Sciex, Framingham,
366 MA).

367

368 **pH-adjusted THB growth**

369 Approximately 30 mL of fresh THB were adjusted to different pH values, measured using
370 a Mettler Toledo FiveEasy pH/MV meter, and sterile-filtered using 0.22 µM syringe filters.
371 A final volume of 200 µL culture medium was aliquoted per well in a flat-bottom 96 well
372 plate (Falcon); culture media were not supplemented with antibiotics. Overnight cultures
373 of GBS strains were used to inoculate the wells to a starting OD_{600nm} 0.02 per well. Plates
374 were incubated for 24 h at 37°C before OD_{600nm} was read using a BioTek MX Synergy 2
375 plate reader. This experiment was performed in biological triplicate.
376
377 **hCMEC cell adherence and invasion assays**
378 Human Cerebral Microvascular Endothelial cells hCMEC/D3 (obtained from Millipore)
379 were grown in EndoGRO-MV complete media (Millipore, SCME004) supplemented with
380 5% fetal bovine serum (FBS) and 1 ng/ml fibroblast growth factor-2 (FGF-2; Millipore).
381 Cells were grown in tissue culture treated 24 well plates and 5% CO_2 at 37°C.
382
383 Assays to determine the total number of bacteria adhered to host cells or intracellular
384 bacteria were performed as described previously (24, 25). Briefly, bacteria were grown to
385 mid log phase (OD_{600nm} 0.4-0.5) and normalized to 1 x 10^8 to infect cell monolayers at a
386 multiplicity of infection (MOI) of 1 (1 x 10^5 CFU per well). The total cell-associated GBS
387 were recovered after 30 min incubation. Cells were washed slowly five times with 500 µL
388 1X PBS (Sigma) and detached by addition of 100 µL of 0.25% trypsin-EDTA solution
389 (Gibco) and incubation for 5 min before lysing the eukaryotic cells with the addition of 400
390 µL of 0.025% Triton X-100 (Sigma) and vigorous pipetting. The lysates were then serially
391 diluted and plated on THB agar and incubated overnight to determine CFU. Bacterial

392 invasion assays were performed as described above except infection plates were
393 incubated for 2 h before incubation with 100 µg gentamicin (Sigma) and 5 µg penicillin
394 (Sigma) supplemented media for an additional 2 h to kill all extracellular bacteria, prior to
395 being trypsinized, lysed, and plated as described. Experiments were performed in
396 biological triplicate with four technical replicates per experiment.
397

398 **Murine model of GBS hematogenous meningitis**

399 All animal experiments were conducted under the approval of the Institutional Animal
400 Care and Use Committee (#00316) at the University of Colorado Anschutz Medical
401 Campus and performed using accepted veterinary standards. The murine meningitis
402 model was performed as previously described (25, 47, 48). Briefly, 7-week-old male
403 CD1 (Charles River) mice were challenged intravenously with 1×10^9 CFU of WT COH1
404 or the isogenic Δ*mprF* mutant. At 72 h post-infection, mice were euthanized and blood,
405 lung and brain tissue were harvested, homogenized, and serially diluted on THB agar
406 plates to determine bacterial CFU.
407

408 **Histology and ELISA**

409 Mouse brain tissue was frozen in OCT compound (Sakura) and sectioned using a
410 CM1950 cryostat (Leica). Sections were stained using hematoxylin and eosin (Sigma)
411 and images were taken using a BZ-X710 microscope (Keyence). Images were analyzed
412 using ImageJ software. Meningeal thickening was quantified from sections taken from
413 three different mice per group, and six images per slide. Meningeal thickening was
414 quantified across two points per image. KC protein from mouse brain homogenates was

415 detected by enzyme-linked immunosorbent assay according to the manufacturer's
416 instructions (R&D systems).
417

418 **Ethics Statement**

419 Animal experiments were approved by the Institutional Animal Care and Use Committee
420 (IACUC) at University of Colorado Anschutz Medical Campus protocol #00316 and were
421 performed using accepted veterinary standards. The University of Colorado Anschutz
422 Medical Campus is AAALAC accredited; and its facilities meet and adhere to the
423 standards in the "Guide for the Care and Use of Laboratory Animals".
424

425 **Conflict of interest**

426 The authors have declared that no conflict of interest exists.
427

428 **Acknowledgements**

429 We thank Kathryn Patras at the University of California San Diego for the CNCTC 10/84
430 strain and Moutusee Islam in Kelli Palmer's lab at The University of Texas at Dallas for
431 *E. faecium* 1,231,410 DNA.
432

433 The work was supported in part by T32 5T32AI052066-18 and F31 AI164674 for H.S.M,
434 the Coordenação de Aperfeiçoamento de Pessoal de Nível Superior, Brazil (CAPES;
435 finance code 001 to J.D.C.M), by grants R01NS116716 and R01AI153332 from the
436 National Institutes of Health (NIH) to K.S.D and associated NIH/NINDS supplement from
437 R01NS116716 to R.V, NIH grant R21AI130666 and the Cecil H. and Ida Green Chair in

Systems Biology Science to K.P, NIH grant R56AI139105 to K.P and Z.G, and NIH grant U54GM069338 to Z.G.

References

1. Roy H. Tuning the properties of the bacterial membrane with aminoacylated phosphatidylglycerol. IUBMB Life. 2009;61:940-53.
2. Adams HM, Joyce LR, Guan Z, Akins RL, Palmer KL. *Streptococcus mitis* and *S. oralis* Lack a Requirement for CdsA, the Enzyme Required for Synthesis of Major Membrane Phospholipids in Bacteria. Antimicrobial agents and chemotherapy. 2017;61:e02552-16.
3. Joyce LR, Guan Z, Palmer KL. Phosphatidylcholine Biosynthesis in Mitis Group Streptococci via Host Metabolite Scavenging. Journal of bacteriology. 2019;201:e00495-19.
4. Wilkinson HW. Group B Streptococcal Infection in Humans. Annual Review of Microbiology. 1978;32:41-57.
5. Doran KS, Nizet V. Molecular pathogenesis of neonatal Group B Streptococcal infection: No longer in its infancy. Molecular Microbiology. 2004;54:23-31.
6. Hall J, Adams NH, Bartlett L, Seale AC, Lamagni T, Bianchi-Jassir F, et al. Maternal Disease With Group B *Streptococcus* and Serotype Distribution Worldwide: Systematic Review and Meta-analyses. Clinical infectious diseases : an official publication of the Infectious Diseases Society of America. 2017;65:S112-S24.
7. Schuchat A. Epidemiology of Group B Streptococcal disease in the United States: shifting paradigms. Clinical microbiology reviews. 1998;11:497-513.
8. Edwards MS, Rench MA, Haffar AA, Murphy MA, Desmond MM, Baker CJ. Long-term sequelae of Group B Streptococcal meningitis in infants. The Journal of pediatrics. 1985;106:717-22.
9. Ohlsson A, Shah VS. Intrapartum antibiotics for known maternal Group B Streptococcal colonization. The Cochrane database of systematic reviews. 2014:CD007467.
10. Armistead B, Oler E, Adams Waldorf K, Rajagopal L. The Double Life of Group B *Streptococcus*: Asymptomatic Colonizer and Potent Pathogen. Journal of Molecular Biology. 2019;431:2914-31.
11. Curtis J, Kim G, Wehr NB, Levine RL. Group B Streptococcal phospholipid causes pulmonary hypertension. Proceedings of the National Academy of Sciences of the United States of America. 2003;100:5087-90.
12. Fischer W. The polar lipids of Group B Streptococci. II. Composition and positional distribution of fatty acids. Biochimica et biophysica acta. 1977;487:89-104.
13. Joyce LR, Guan Z, Palmer KL. *Streptococcus pneumoniae*, *S. pyogenes* and *S. agalactiae* membrane phospholipid remodelling in response to human serum. Microbiology (Reading). 2021;167(5).

478 14. Doran KS, Engelson EJ, Khosravi A, Maisey HC, Fedtke I, Equils O, et al. Blood-
479 brain barrier invasion by Group B *Streptococcus* depends upon proper cell-surface
480 anchoring of lipoteichoic acid. The Journal of clinical investigation. 2005;115:2499-507.
481 15. Slavetinsky C, Kuhn S, Peschel A. Bacterial aminoacyl phospholipids -
482 Biosynthesis and role in basic cellular processes and pathogenicity. Biochimica et
483 biophysica acta Molecular and cell biology of lipids. 2017;1862:1310-8.
484 16. Peschel A, Jack RW, Otto M, Collins LV, Staubitz P, Nicholson G, et al.
485 *Staphylococcus aureus* resistance to human defensins and evasion of neutrophil killing
486 via the novel virulence factor MprF is based on modification of membrane lipids with L-
487 lysine. Journal of Experimental Medicine. 2001;193:1067-76.
488 17. Weidenmaier C, Peschel A, Kempf VA, Lucindo N, Yeaman MR, Bayer AS.
489 DltABCD- and MprF-mediated cell envelope modifications of *Staphylococcus aureus*
490 confer resistance to platelet microbicidal proteins and contribute to virulence in a rabbit
491 endocarditis model. Infect Immun. 2005;73(12):8033-8.
492 18. Kuypers JM, Heggen LM, Rubens CE. Molecular analysis of a region of the
493 Group B *Streptococcus* chromosome involved in type III capsule expression. Infection
494 and immunity. 1989;57:3058-65.
495 19. Lancefield RC, McCarty M, Everly WN. Multiple mouse-protective antibodies
496 directed against Group B Streptococci. Special reference to antibodies effective against
497 protein antigens. The Journal of experimental medicine. 1975;142:165-79.
498 20. Wilkinson HW. Nontypable Group B Streptococci isolated from human sources.
499 Journal of clinical microbiology. 1977;6:183-4.
500 21. Smith CA, O'Maille G, Want EJ, Qin C, Trauger SA, Brandon TR, et al. METLIN:
501 a metabolite mass spectral database. Ther Drug Monit. 2005;27(6):747-51.
502 22. Sud M, Fahy E, Cotter D, Brown A, Dennis EA, Glass CK, et al. LMSD: LIPID
503 MAPS structure database. Nucleic Acids Res. 2007;35(Database issue):D527-32.
504 23. Roy H, Ibba M. RNA-dependent lipid remodeling by bacterial multiple peptide
505 resistance factors. Proceedings of the National Academy of Sciences of the United
506 States of America. 2008;105:4667-72.
507 24. Deng L, Spencer BL, Holmes JA, Mu R, Rego S, Weston TA, et al. The Group B
508 Streptococcal surface antigen I/II protein, BspC, interacts with host vimentin to promote
509 adherence to brain endothelium and inflammation during the pathogenesis of
510 meningitis. PLoS pathogens. 2019;15:e1007848.
511 25. Spencer BL, Deng L, Patras KA, Burcham ZM, Sanches GF, Nagao PE, et al.
512 Cas9 contributes to Group B Streptococcal colonization and disease. Frontiers in
513 Microbiology. 2019;10:1-15.
514 26. Faralla C, Metruccio MM, De Chiara M, Mu R, Patras KA, Muzzi A, et al. Analysis
515 of two-component systems in Group B *Streptococcus* shows that RgfAC and the novel
516 FspSR modulate virulence and bacterial fitness. mBio. 2014;5(3):e00870-14.
517 27. Spencer BL, Chatterjee A, Duerkop BA, Baker CJ, Doran KS. Complete Genome
518 Sequence of Neonatal Clinical Group B Streptococcal Isolate CJB111. Microbiology
519 resource announcements. 2021;10.
520 28. Mu R, Cutting AS, Del Rosario Y, Villarino N, Stewart L, Weston TA, et al.
521 Identification of CiaR Regulated Genes That Promote Group B Streptococcal Virulence
522 and Interaction with Brain Endothelial Cells. PLoS One. 2016;11(4):e0153891.

523 29. Ernst CM, Kuhn S, Slavetinsky CJ, Krismer BB, Heilbronner S, Gekeler C, et al.
524 The Lipid-Modifying Multiple Peptide Resistance Factor Is an Oligomer Consisting of
525 Distinct Interacting Synthase and Flippase subunits. mBio. 2015;6:1-9.
526 30. Roy H, Ibba M. Broad range amino acid specificity of RNA-dependent lipid
527 remodeling by multiple peptide resistance factors. Journal of Biological Chemistry.
528 2009;284:29677-83.
529 31. Hebecker S, Krausze J, Hasenkampf T, Schneider J, Groenewold M, Reichelt J,
530 et al. Structures of two bacterial resistance factors mediating tRNA-dependent
531 aminoacylation of phosphatidylglycerol with lysine or alanine. Proceedings of the
532 National Academy of Sciences of the United States of America. 2015;112:10691-6.
533 32. Lennarz WJ, Nesbitt JA, Reiss J. The participation of sRNA in the enzymatic
534 synthesis of O-L-lysyl phosphatidylgylcerol in *Staphylococcus aureus*. Proceedings of
535 the National Academy of Sciences of the United States of America. 1966;55:934-41.
536 33. Saar-Dover R, Bitler A, Nezer R, Shmuel-Galia L, Firon A, Shimoni E, et al. D-
537 alanylation of lipoteichoic acids confers resistance to cationic peptides in Group B
538 *Streptococcus* by increasing the cell wall density. PLoS pathogens. 2012;8:e1002891.
539 34. Surve MV, Anil A, Kamath KG, Bhutda S, Sthanam LK, Pradhan A, et al.
540 Membrane Vesicles of Group B *Streptococcus* Disrupt Feto-Maternal Barrier Leading to
541 Preterm Birth. PLOS Pathogens. 2016;12:e1005816.
542 35. Reichmuth AM, Oberli MA, Jaklenec A, Langer R, Blankschtein D. mRNA
543 vaccine delivery using lipid nanoparticles. Ther Deliv. 2016;7(5):319-34.
544 36. Hafez IM, Maurer N, Cullis PR. On the mechanism whereby cationic lipids
545 promote intracellular delivery of polynucleic acids. Gene Ther. 2001;8(15):1188-96.
546 37. Van De Rijn I, Kessler RE. Growth characteristics of Group A Streptococci in a
547 new chemically defined medium. Infection and Immunity. 1980;27:444-8.
548 38. Chang JC, LaSarre B, Jimenez JC, Aggarwal C, Federle MJ. Two Group A
549 Streptococcal peptide pheromones act through opposing rgg regulators to control
550 biofilm development. PLoS Pathogens. 2011;7:e1002190.
551 39. Gupta R, Shah P, Swiatlo E. Differential gene expression in *Streptococcus*
552 *pneumoniae* in response to various iron sources. Microbial Pathogenesis. 2009;47:101-
553 9.
554 40. Granok AB, Parsonage D, Ross RP, Caparon MG. The RofA binding site in
555 *Streptococcus pyogenes* is utilized in multiple transcriptional pathways. Journal of
556 bacteriology. 2000;182:1529-40.
557 41. Jeng A, Sakota V, Li Z, Datta V, Beall B, Nizet V. Molecular genetic analysis of a
558 Group A *Streptococcus* operon encoding serum opacity factor and a novel fibronectin-
559 binding protein, SfbX. J Bacteriol. 2003;185(4):1208-17.
560 42. Hooven TA, Bonakdar M, Chamby AB, Ratner AJ. A Counterselectable Sucrose
561 Sensitivity Marker Permits Efficient and Flexible Mutagenesis in *Streptococcus*
562 *agalactiae*. Applied and environmental microbiology. 2019;85:1-13.
563 43. Holo H, Nes IF. High-frequency transformation, by electroporation, of
564 *Lactococcus lactis* subsp. *cremoris* grown with glycine in osmotically stabilized media.
565 Applied and Environmental Microbiology. 1989;55:3119-23.
566 44. Framson PE, Nittayajarn A, Merry J, Youngman P, Rubens CE. New genetic
567 techniques for Group B Streptococci: High-efficiency transformation, maintenance of

568 temperature-sensitive pWV01 plasmids, and mutagenesis with Tn917. Applied and
569 Environmental Microbiology. 1997;63:3539-47.
570 45. Tan BK, Bogdanov M, Zhao J, Dowhan W, Raetz CRH, Guan Z. Discovery of a
571 cardiolipin synthase utilizing phosphatidylethanolamine and phosphatidylglycerol as
572 substrates. Proceedings of the National Academy of Sciences. 2012;109:16504-9.
573 46. Li C, Tan BK, Zhao J, Guan Z. In vivo and in vitro synthesis of
574 phosphatidylglycerol by an *Escherichia coli* cardiolipin synthase. Journal of Biological
575 Chemistry. 2016;291:25144-53.
576 47. Kim BJ, Hancock BM, Bermudez A, Del Cid N, Reyes E, van Sorge NM, et al.
577 Bacterial induction of Snail1 contributes to blood-brain barrier disruption. The Journal of
578 clinical investigation. 2015;125:2473-83.
579 48. Banerjee A, Kim BJ, Carmona EM, Cutting AS, Gurney MA, Carlos C, et al.
580 Bacterial Pili exploit integrin machinery to promote immune activation and efficient
581 blood-brain barrier penetration. Nature communications. 2011;2:462.

582

583

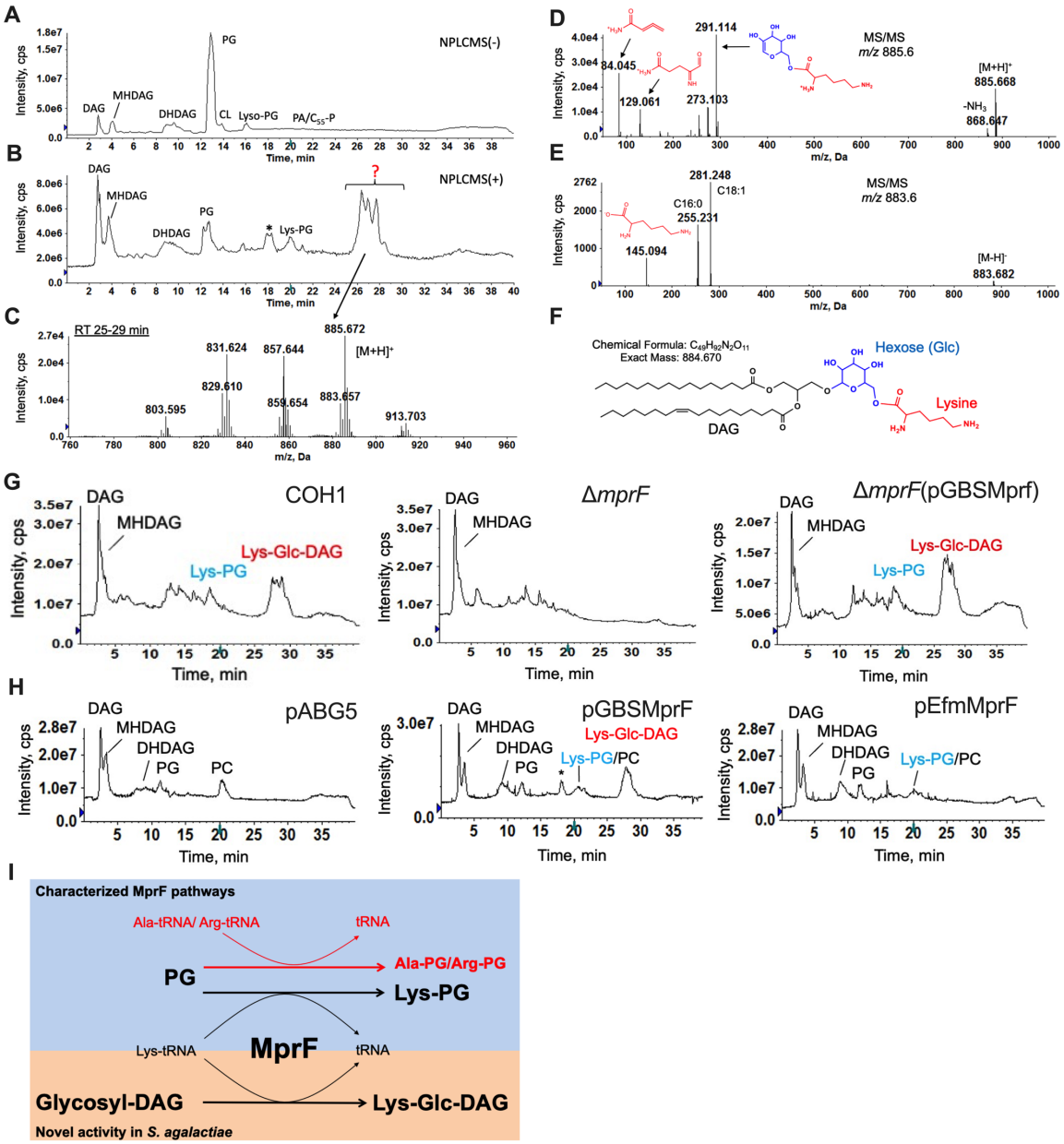

Fig 1. Lipidomic profiling of GBS and identification of Lys-Glc-DAG synthesized by MprF. Total ion chromatogram (TIC) of LC/MS in A) negative ion mode, B) positive ion mode shows a major unknown lipid eluting at ~25-29 min. C) Positive ESI/MS showing the $[M+H]^+$ ions of the unknown lipid. D) Positive ion MS/MS spectrum of $[M+H]^+$ at *m/z* 885.6 and E) negative ion MS/MS spectrum of $[M-H]^-$ at *m/z* 883.6 of the unknown lipid. F) Lys-Glc-DAG (16:0/18:1) is proposed as the structure of the unknown lipid. G) TIC showing loss of Lys-Glc-DAG and Lys-PG in COH1Δ*mprF* which is present when *mprF* is complemented *in trans*. H) Lys-Glc-DAG and Lys-PG is only present in *S. mitis* when expressing GBS *mprF* compared to Lys-PG only when expressing *E. faecium mprF*. "*" denotes methylcarbamate of Lys-Glc-DAG, an extraction artifact due to the use of chloroform. I) Biosynthetic pathways involving MprF.

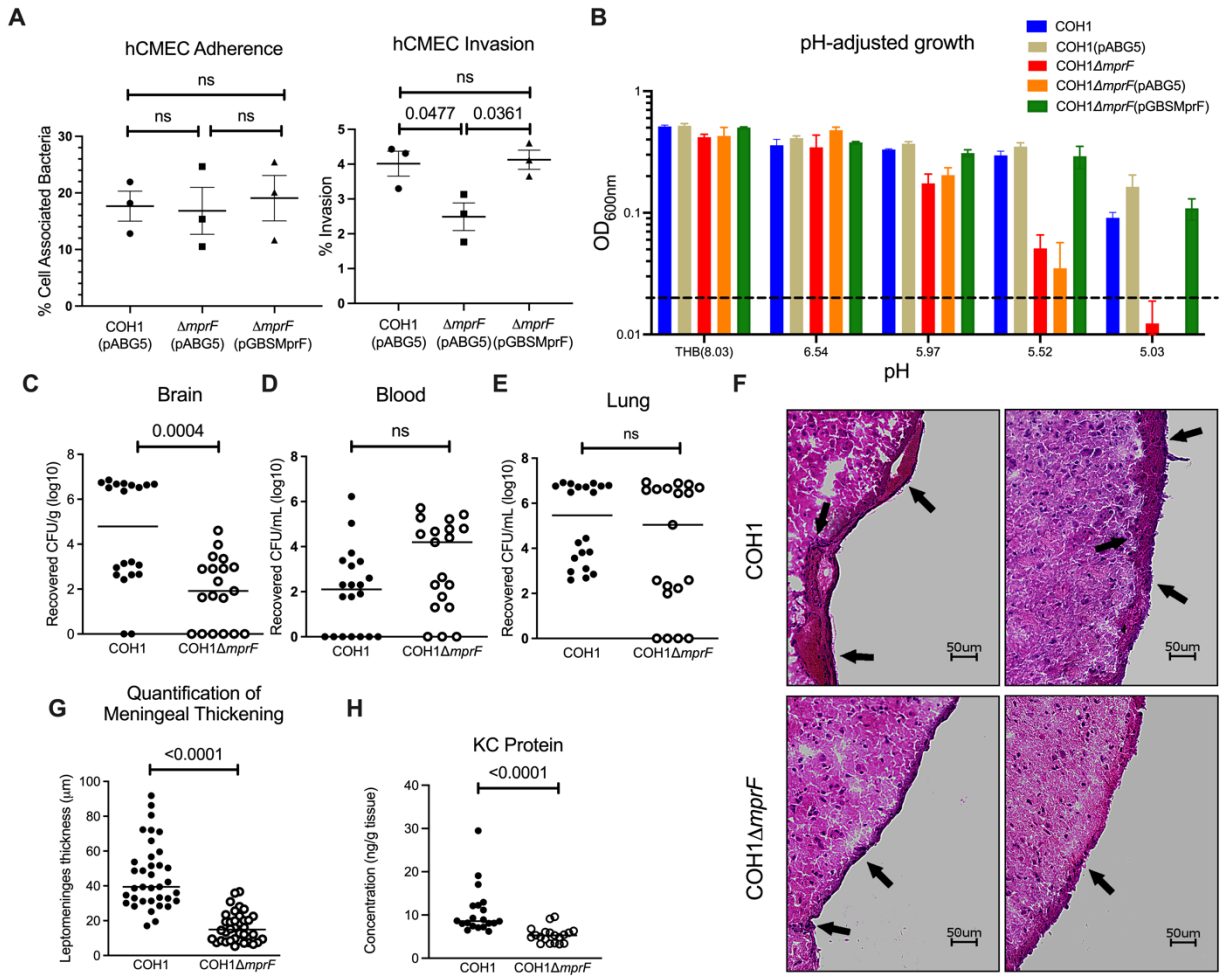

Fig 2. Contribution of lysine lipids to meningitis pathogenesis. A) *In vitro* assays for adherence and invasion of hCMEC cells indicates *mprF* contributes to invasion but not adherence to brain endothelium (the mean of each biological replicate is displayed, comprised of 4 replicate wells per biological replicate, mean and SEM). B) pH-adjusted medium growth indicates Δ*mprF* cannot survive in low pH conditions, mean and SD. Groups of CD-1 mice were injected intravenously with COH1 WT or COH1Δ*mprF* strains and bacterial counts were assessed in the C) brain, D) blood, and E) lung after 72h. Representative data from 2 independent experiments are shown (WT, n = 20; Δ*mprF*, n = 19). F) Hematoxylin-eosin-stained brain sections from representative mice infected with WT (top) or Δ*mprF* mutant (bottom); arrows indicate meningeal thickening and leukocyte infiltration. G) Quantification of meningeal thickening using ImageJ. H) KC chemokine production measured by ELISA. Panels C, D, E, G, and H) median indicated. Statistical analyses performed using GraphPad Prism: A) One-way ANOVA with Tukey's multiple comparisons test; C, D, F) unpaired two-tailed t-test; E, G) Mann-Whitney U test; p-values indicated; ns, no significance (p-value > 0.05).

614 **Supplemental Figures, and Tables**

615 **Identification of a novel cationic glycolipid in *Streptococcus agalactiae* that**

616 **contributes to brain entry and meningitis**

617

618 Luke R. Joyce[a,b], Haider S. Manzer[b], Jéssica da C. Mendonça[b,c], Ricardo Villarreal[b],
619 Prescilla E. Nagao[c] , Kelly S. Doran[b#,] Kelli L. Palmer[a#], and Ziqiang Guan[d#]

620

621 [a]Department of Biological Sciences, The University of Texas at Dallas, Richardson, TX,

622 75080

623 [b]Department of Immunology and Microbiology, University of Colorado School of

624 Medicine, Aurora, CO, 80045

625 [c]Rio de Janeiro State University, Roberto Alcântara Gomes Biology Institute, Rio de

626 Janeiro, RJ, Brazil

627 [d]Department of Biochemistry, Duke University Medical Center, Durham, NC, 27710

628

629

630 [#]Corresponding authors

631

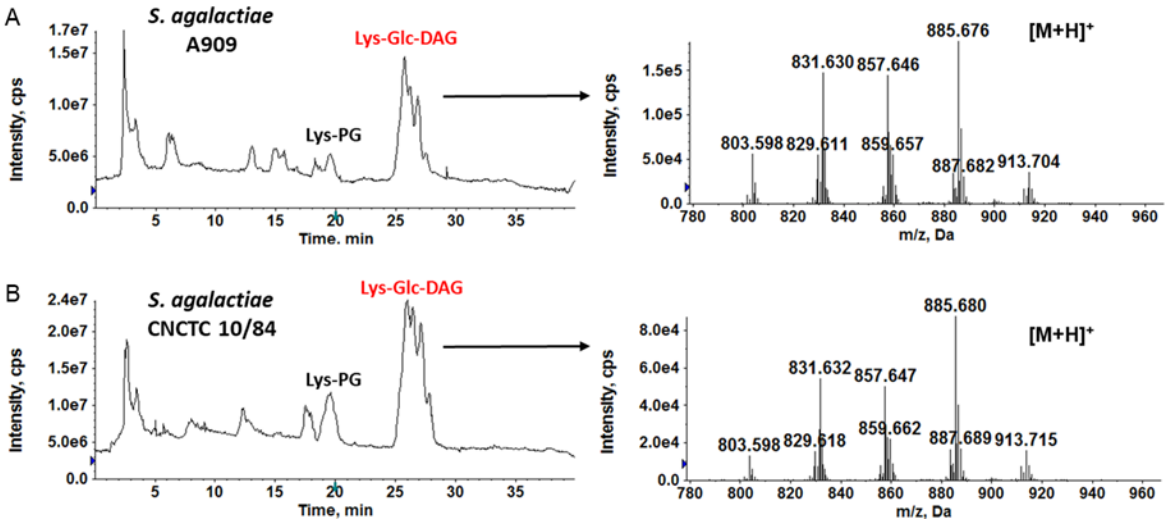

632

633 **S1 Fig. Detection of Lys-PG and Lys-Glc-DAG in *S. agalactiae* A909 and *S.***
634 ***agalactiae* CNCTC 10/84.** Positive TICs (left panels) showing the presence of Lys-PG
635 and Lys-Glc-DAG in S*. agalactiae* A909 and S*. agalactiae* CNCTC 10/84. Mass spectra
636 (right panels) show the $[M+H]^+$ ions of Lys-Glc-DAG.

637

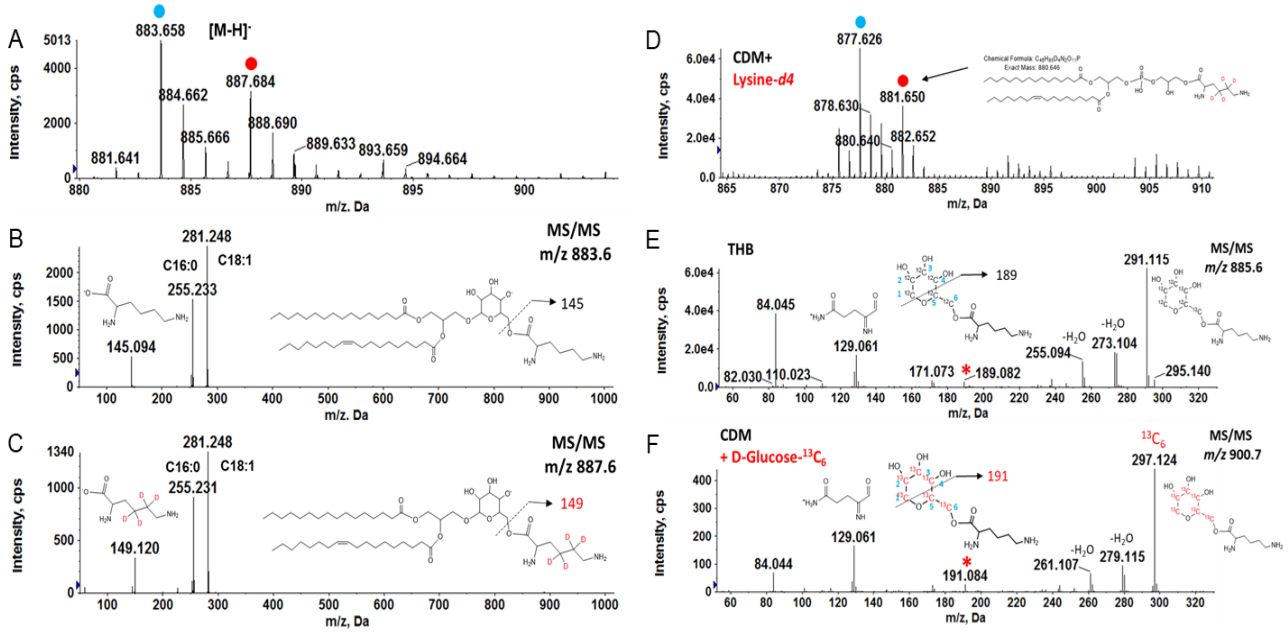

S2 Fig. Isotopic incorporation of deuterated lysine and ^{13}C-labeled glucose into Lys-Glc-DAG and Lys-PG. The lipid extracts of *S. agalactiae* COH1 cultured in DM, DM supplemented with 450 μM L-lysine-*d4* (4,4,5,5-D4), or in DM containing 0.5% w/v D-Glucose (U-$^{13}C_6$) were analyzed by LC-ESI/MS in the positive ion mode. A) Negative ESI/MS of $[M-H]^-$ ions of major Lys-Glc-DAG species in *S. agalactiae* COH1 when cultured in DM supplemented with lysine-*d4*. The incorporation of lysine-*d4* into Lys-Glc-DAG is evidenced by an upward *m/z* shift of 4 Da of the $[M-H]^-$ ion (from *m/z* 883 to *m/z* 887). B) MS/MS of $[M-H]^-$ at *m/z* 883.6 produces a deprotonated lysine residue at *m/z* 145. C) MS/MS of $[M-H]^-$ at *m/z* 887.6 produces a deprotonated lysine-*d4* residue at *m/z* 149. D) $[M+H]^+$ ions of major Lys-PG species in *S. agalactiae* COH1 cultured in DM supplemented with lysine-*d4.* The incorporation of lysine-*d4* in Lys-PG is evidenced by an upward *m/z* shift of 4 Da from unlabeled Lys-PG (blue dot) to labeled Lys-PG (red dot). E) MS/MS of 885.6. A major product ion at *m/z* 291.1 is derived from glucose-lysine residue. F) MS/MS of *m/z* 900.7 (containing fifteen ^{13}C atoms). The presence of *m/z* 297.1 (with 6 Da shift) is consistent with glucose in Lys-Glc-DAG is replaced with D-Glucose (U-$^{13}C_6$). The other nine ^{13}C atoms are incorporated into the DAG portion of Lys-Glc-DAG. Furthermore, MS/MS data indicate that lysine is linked to the C6 position of glucose by the fragmentation schemes for forming *m/z* 189 ion from the unlabeled Lys-Glc-DAG and *m/z* 191 ion from the ^{13}C-labeled Lys-Glc-DAG.

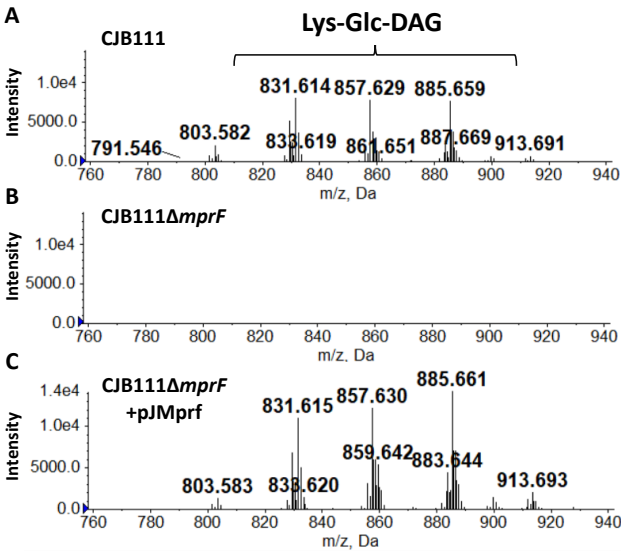

S3 Fig. Positive ion mass spectra of retention time 27-29 minutes of hypervirulent CJB111 strain. Lys-Glc-DAG is present in the membrane of WT CJB111 (A). Deletion of *mprF* from CJB111 genome results in loss of Lys-Glc-DAG from the membrane (B). *MprF* complemented *in trans* reestablishes Lys-Glc-DAG back into the membrane (C).

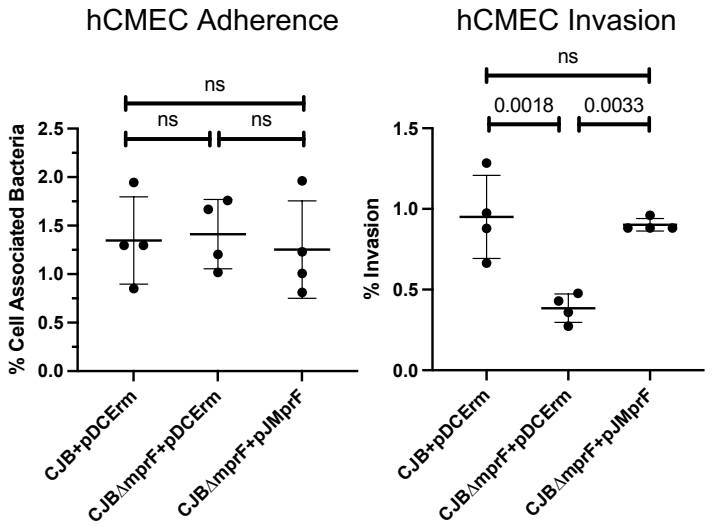

S4 Fig. *In vitro* hCMEC adhesion and invasion of CJB111 strains. *In vitro* assays for adherence and invasion of hCMEC cells indicates *mprF* contributes to invasion but not adherence to brain endothelium. Data indicates the percentage of the initial inoculum that was recovered. Experiments were performed three times with each condition in quadruplicate. Data from one representative experiment is shown, mean and standard deviation indicated. One-Way ANOVA with Tukey's multiple comparisons statistical test was used. P-values indicated; ns, not significant.

673 **S1 Table. Observed and calculated exact masses of the $[M+H]^+$ ions of Lys-Glc-**
674 **DAG molecular species in *S. agalactiae* COH1.**

Lys-Glc-DAG[1]	$[M+H]^+$	
	Observed mass	**Exact mass**
C28:1	801.575	801.583
C28:0	803.595	803.599
C30:1	829.610	829.615
C30:0	831.624	831.630
C32:2	855.623	855.630
C32:1	857.644	857.646
C34:2	883.657	883.622
C34:1	885.672	885.677
C36:2	911.686	911.693
C36:1	913.703	913.709

675

676 [1]The numbers before and after colons indicate the total acyl chain carbon atoms and
677 double bonds, respectively.

678 **S2 Table. Strains and plasmids used in this study.**

Organism	Strain	Description	Ref
S. agalactiae	ATCC BAA-1176 (COH1)	Wild-type *S. agalactiae* strain, serotype III	(1)
	COH1Δ*mprF*	*mprF* (GBSCOH1_1931) deletion strain	This work
	COH1Δ*mprF(*pABG5)	Empty vector control strain	This work
	COH1Δ*mprF*(pGBSMprf)	Expresses GBS *mprF* from P_{prtF} in pABG5Δ*phoZ*	This work
	COH1(pABG5)	Empty vector control	This work
	CJB111	Wilt-type *S. agalactiae* strain, serotype V	(2, 3)
	CJB111Δ*mprF*	*mprF* (ID870_10050) deletion strain	This work
	CJB111Δ*mprF*(pDCErm)	Empty vector control strain	This work
	CJB111Δ*mprF*(pJMprF)	Expresses GBS *mprF* in pDCErm	This work
	ATCC BAA-1138 (A909)	Wild-type *S. agalactiae* strain, serotype Ia	(4)
	CNCTC 10/84	Wild-type *S. agalactiae* strain, serotype V. Obtained from Dr. K Patras, UCSD	(5, 6)
S. mitis	ATCC 49456	Wild-type *S. mitis* type strain, also known as NCTC 12261	(7)
	ATCC 49456(pABG5)	Empty vector control	This work
	ATCC 49456(pGBSMprF)	Expresses GBS *mprF* from P_{prtF} in pABG5Δ*phoZ*	This work
	ATCC 49456(pEfmMprF)	Expresses *E. faecium mprF1* from P_{prtF} in pABG5Δ*phoZ*	This work
E. coli	DH5α	Plasmid cloning host; F^-, φ80*lac*ZΔM15, *rec*A1, *end*A1, *hsd*R17, *pho*A, *s up*E44, λ^- *thi*-1, *gyr*A96, *rel*A1	(8)
	DH5α(pABG5)	Empty vector control	This work
	MC1061	Plasmid cloning host; F^-, araD139, Δ(araABC-leu)7696, Δ(lac)X74, galU, galK, hsdR2, (r_K^- m_K^+), mcrB1, rpsL, (Str^r)	(9)
	MC1061(pDCErm)	Empty vector control	This work
	DH5α(pGBSMprF)	Expresses COH1 *mprF* (GBSCOH1_1931) from P_{prtF} in pABG5Δ*phoZ*	This work

	DH5α(pEfmMprF)	Expresses *E. faecium mprF1* from P_{prtF} in pABG5Δ*phoZ*	This work
	DH5α(pMBMprFKO)	Allelic exchange plasmid containing ~2 kb sequence flanking GBSCOH1_1931	This work
	MC1061(pJMprFKO)	Allelic exchange plasmid containing ~2 kb sequence flanking ID870_10050	This work
	MC1061(pJMprF)	Expresses CJB11 *mprF* from $P_{tetM/erm}$ in pDCErm	This work
E. faecium	1,231,410	Wild type *E. faecium* strain	(10)

Plasmid	**Description**	**Ref**
pABG5Δ*phoZ*	Constitutive expression vector for streptococci with the P_{prtF} promoter. Confers kanamycin resistance. Referred to as pABG5 throughout the text	(11)
pGBSMprF	pABG5Δ*phoZ* expressing COH1 *mprF* (GBSCOH1_1931) from P_{prtF}	This work
pEfmMprF	pABG5Δ*phoZ* expressing *E. faecium* 1,231,410 *mprF1* (EFTG_00601) from P_{prtF}	This work
pMBSacB	Allelic exchange plasmid for *S. agalactiae*. Confers erythromycin resistance and sucrose sensitivity	(12)
pMBMprFKO	Knockout plasmid containing ~2 kb sequence flanking GBSCOH1_1931	This work
pJMprFKO	Knockout plasmid containing ~2 kb sequence flanking ID870_10050	This work
pDCErm	Consitituitive expression vector for streptococcus from $P_{tetM/erm}$	(13)
pJMprF	pDCErm expressing CJB111 *mprF* (ID870_10050)	This work

679

680

681 **S3 Table. Primers used in this study.**

Primer	5' – 3' sequence	Use
GBS_MprF_F	GAGAGGTCCCTTTCCTTGAAAAAGCTAATTGAAAAAGTC	Amplify GBSCOH1_1931 for Gibson assembly
GBS_MprF_R	ACCAATACCTTTATCTTATTTAACAATCTTAATTTTACTATC	Amplify GBSCOH1_1931 for Gibson assembly
Faec_MprF1_F	GAGAGGTCCCTTTCCTTGTTAAAAAATACCATACAATG	Amplify EFTG_00601 for Gibson assembly
Faec_MprF1_R	ACCAATACCTTTATCTTAATACTTTCTTCGTATCC	Amplify EFTG_00601 for Gibson assembly
MpF_SacII	ACGTCACCGCGGTTGAAAAAGCTAATTGAAAAAGTC	Amplify CJB111 *mprF* ID870_10050 for ligation
MpR_BamHI	ACGTCAGGATCCTTATTTAACAATCTTAATTTTACTATC	Amplify CJB111 *mprF* ID870_10050 for ligation
pABG5-5'	GGAAAGGGACCTCTCTTCCTAAAC	Linearize pABG5Δ*phoZ* for Gibson assembly
pABG5-3'	GATAAAGGTATTGGTAAATAACAAA	Linearize pABG5Δ*phoZ* for Gibson assembly
	Expression plasmid sequencing	
GBS_S1	GAATGGAATAATATAGTAGGCT	For sequencing pGBSMprF/pJMprF, amplifies with pABG5_Fup2/ pF
GBS_S2	GATTGTATCCCTTATTCC	For sequencing pGBSMprF/pJMprF, amplifies with GBS_S3
GBS_S3	CGATTCAATAGCTTCAC	For sequencing pGBSMprF/pJMprF, amplifies with GBS_S2
GBS_S4	GATAAAAGGCTCTACTGG	For sequencing pGBSMprF/pJMprF, amplifies with pABG5_FDwn/pR
pABG5_FDwn	CCAATAATAATGACTAGAGAAG	For pABG5 plasmid insert sequencing
pABG5_Fup2	CAAAAGGTTTCGACTTTTCACC	For pABG5 plasmid insert sequencing
EF1_S1	GAATAACGCTGATCAAAAGT	For sequencing pEfmMprF1, amplifies with pABG5_Fup2
EF1_S2	TGCCAAGAGAAATAGTC	For sequencing pEfmMprF1, amplifies with EF1_S3
EF1_S3	ACAATCTCTTCGCTTG	For sequencing pEfmMprF1, amplifies with EF1_S2
EF1_S4	CCAACTGTTCTTCTCCAA	For sequencing pEfmMprF1, amplifies with pABG5_FDwn
pF	AGCGCTAGGAGGAAAC	For pDCErm plasmid insert sequencing
pR	CCCATGCCATCTCCAATC	For pDCErm plasmid insert sequencing
GBSCOH1_1931 knockout plasmid construction, sequencing, and integration screening		
Mp1F_PstI	ACGTCACTGCAGTTCAATTAGCTTTTTCAACAATTTC	Amplifies upstream fragment from within GBSCOH1_1931/ID870_10050 leaving 6 codons, with Mp1R_XhoI
Mp1R_XhoI	ACGTCACTCGAGGCTGTTTATGGTGCTTTG	5' most primer of upstream fragment, amplifies with Mp1F_PstI
Mp2F_XbaI	ACGTCATCTAGAGAAAAGGCTAGATTACGAAC	3' most primer of downstream fragment, amplifies with Mp2R_PstI
Mp2R_PstI	ACGTCACTGCAGGTTAAATAAGCTTTATTTGGCA	Amplifies downstream fragment leaving 2 codons and stop codon of GBSCOH1_1931/ID870_10050, with Mp2F_XbaI
T7 promoter	TAATACGACTCACTATAGGG	Amplifies with MpS5F below to sequence plasmid, amplifies with T3 promoter for insert screening and plasmid presence
T3 promoter	AATTAACCCTCACTAAAGGG	Amplifies with MpS3R below, amplifies with T7 promoter for insert screening and plasmid presence
Int_F	GCTAATTGAACTGCAGGTTAAATAAG	Anneals at *mprF* knockout site, amplifies with Out_R for single integration screening

Out_R	GCTATTATATTTAGTGGTTTAATTGG	Anneals outside recombination arms, amplifies with Int_F, for single integration screening
Genomic knockout region sequencing		
MpS3F	CATTAGCTAGTCTTATCGGAG	Anneals outside integration arms, amplifies with MpS3R
MpS3R	ACAGCTACTTGGTAGTTCA	Amplifies with MpS3F
MpS4F	GCTACTAAGGCAAGATACG	Amplifies with MpS4R, knockout screening and plasmid sequencing primer
MpS4R	ATGGTCAGCGATGGTG	Amplifies with MpS4F, knockout screening and plasmid sequencing primer
MpS5F	CATAAGCGAAATAACTTGAG	Amplifies with MpS5R
MpS5R	GTATACAACGGCTTGATTGG	Anneals outside integration arms, amplifies with MpS5F

682

683

References

1. Kuypers JM, Heggen LM, Rubens CE. Molecular analysis of a region of the Group B *Streptococcus* chromosome involved in type III capsule expression. Infection and immunity. 1989;57:3058-65.
2. Faralla C, Metruccio MM, De Chiara M, Mu R, Patras KA, Muzzi A, et al. Analysis of two-component systems in group B Streptococcus shows that RgfAC and the novel FspSR modulate virulence and bacterial fitness. mBio. 2014;5(3):e00870-14.
3. Spencer BL, Chatterjee A, Duerkop BA, Baker CJ, Doran KS. Complete Genome Sequence of Neonatal Clinical Group B Streptococcal Isolate CJB111. Microbiology resource announcements. 2021;10.
4. Lancefield RC, McCarty M, Everly WN. Multiple mouse-protective antibodies directed against Group B Streptococci. Special reference to antibodies effective against protein antigens. The Journal of experimental medicine. 1975;142:165-79.
5. Hooven TA, Randis TM, Daugherty SC, Narechania A, Planet PJ, Tettelin H, et al. Complete Genome Sequence of *Streptococcus agalactiae* CNCTC 10/84, a Hypervirulent Sequence Type 26 Strain. Genome announcements. 2014;2:e01338-14.
6. Wilkinson HW. Nontypable Group B Streptococci isolated from human sources. Journal of clinical microbiology. 1977;6:183-4.
7. Kilian M, Mikkelsen L, Henrichsen J. Taxonomic Study of Viridans Streptococci: Description of *Streptococcus gordonii* sp. nov. and Emended Descriptions of *Streptococcus sanguis* (White and Niven 1946), *Streptococcus oralis* (Bridge and Sneath 1982), and *Streptococcus mitis* (Andrewes and Horder 1906). International Journal of Systematic Bacteriology. 1989;39:471-84.
8. Taylor RG, Walker DC, McInnes RR. *E. coli* host strains significantly affect the quality of small scale plasmid DNA preparations used for sequencing. Nucleic acids research. 1993;21:1677-8.
9. Casadaban MJ, Cohen SN. Analysis of gene control signals by DNA fusion and cloning in Escherichia coli. J Mol Biol. 1980;138(2):179-207.
10. Palmer KL, Carniol K, Manson JM, Heiman D, Shea T, Young S, et al. High-quality draft genome sequences of 28 *Enterococcus* sp. isolates. Journal of bacteriology. 2010;192:2469-70.
11. Granok AB, Parsonage D, Ross RP, Caparon MG. The RofA binding site in *Streptococcus pyogenes* is utilized in multiple transcriptional pathways. Journal of bacteriology. 2000;182:1529-40.
12. Hooven TA, Bonakdar M, Chamby AB, Ratner AJ. A Counterselectable Sucrose Sensitivity Marker Permits Efficient and Flexible Mutagenesis in *Streptococcus agalactiae*. Applied and environmental microbiology. 2019;85:1-13.
13. Jeng A, Sakota V, Li Z, Datta V, Beall B, Nizet V. Molecular genetic analysis of a group A Streptococcus operon encoding serum opacity factor and a novel fibronectin-binding protein, SfbX. J Bacteriol. 2003;185(4):1208-17.